A Platinum Open Access Journal for Organic Chemistry

Review

Free to Authors and Readers | DOAJ Seal | *Arkivoc* **2026** (2) 202612599

Supported gold nanoparticles – synthesis, characterization and applications in the multistep synthesis of valuable chemicals

Kristina Plevova* and Sylvain Antoniotti

Université Côte d'Azur, CNRS, Institut de Chimie de Nice
Parc Valrose, 06108 Nice cedex 2, FRANCE
Email: kristina.plevova@univ-cotedazur.fr

Received 04-24-2026 **Accepted** 08-23-2026 **Published on line** 09-15-2026

Abstract

Supported gold nanoparticles have emerged as powerful catalysts for complex multistep transformations. This review discusses synthetic approaches for preparing supported gold nanoparticles, as well as key methods used to characterize the particle sizes and morphologies, the metal–support interactions and the degree of oxidation. The impact of these factors on catalytic activity is also discussed. Special attention is then given to their application in multistep synthesis. Current challenges and perspectives for their use in complex synthetic processes are also discussed.

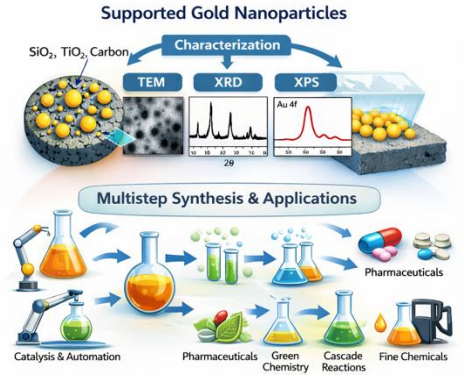

(generated with AI)

Keywords: supported gold nanoparticles; multistep synthesis; domino and cascade reactions; green chemistry

Table of Contents

1. Introduction

Supported gold nanoparticles (Au NPs) have attracted attention in recent decades as a class of highly active heterogeneous catalysts for a wide range of chemical transformations, uniting the fields of nanoscience, catalysis, and the development of synthetic methods in organic synthesis. Historically, bulk gold was considered catalytically inert due to its noble metal character,[1] but this interpretation dramatically changed after

pioneering studies showed that nanogold particles with sizes below 5 nm could exhibit remarkable catalytical activity, mainly in oxidation and reduction reactions.[2-6]

Supported Au NPs have been successfully applied in different chemical transformations such as selective oxidation,[3, 7-11] hydrogenation,[12-14] the water-gas shift reaction,[15-17] acetylene hydrochlorination,[18-19] C–C coupling reactions,[20-22] reduction of NO to N_2,[23-24] direct synthesis of H_2O_2[6] and several others.[25-28] More recently, they have also found applications in more sophisticated tandem processes. The high catalytic activity of supported Au NPs, often occurring under relatively mild reaction conditions, as compared with conventional heterogeneous processes, combined with a high recyclability potential, make them very attractive for sustainable and green chemistry applications.

Although several review articles have previously discussed the synthesis, characterization, and catalytic properties of supported Au NPs, most of them focusing mainly on catalyst preparation, the role of the support, or individual catalytic transformations. Less attention has been paid to the use of supported Au NPs in one-pot and/or tandem multistep organic synthesis approaches to synthesize value-added chemicals. During the last decade, significant progress has been achieved in the rational design of supported Au NPs catalysts, advanced characterization methods, and the understanding of synergistic interactions between active sites, which has enabled increasingly efficient tandem and multicatalytic transformations. The present review, provides a comprehensive overview of the synthesis and characterization of supported Au NPs, discusses the different factors that can influence their catalytic activity and highlights their applications in one-pot and/or tandem multistep organic synthesis of valuable chemical molecules. It therefore fills an important gap in the current literature and identifies opportunities for the further development of Au-based heterogeneous catalysts.

2. Synthesis of Supported Gold Nanoparticles

Gold nanoparticles (Au NPs), can be synthesized using three main approaches could be used: 1) chemical,[29] 2) physical[30] and 3) biological methods.[31-32] To increase the thermal or chemical stability of Au NPs, different inorganic compounds have been used as effective supports.

Many metal nanoparticles supported on various inorganic supports are commercially available, but can also be easily obtained by using reported preparation methods.[33-34] Various inorganic compounds have been employed as effective supports for the preparation and stabilization of Au NPs, including titanium oxide, alumina, cerium oxide, magnesium oxide, silica, ferric oxide or zeolites. Resins and polymers can also be used as organic supports, although their physicochemical binding properties are different.

Several preparation methods can be applied to synthesize Au NPs on these supports, and the most important approaches found in the literature are: *1. Impregnation, 2. Sol-Immobilization, 3. Co-Precipitation, 4. Deposition and Precipitation, 5. Liquid-Phase Reductive Deposition, 6. Photochemical Deposition, 7. Ion-Exchange, 8. Ultrasonication.*

2.1. Impregnation, double impregnation, wet impregnation and incipient wetness impregnation techniques

Impregnation methods are among the most commonly used methods for the synthesis of supported metal nanoparticles, mainly because of their versatility, simplicity and low cost. First, a solution of metal salt ($HAuCl_4$, $AuCl_3$, Au_2Cl_6) is prepared, followed by impregnation onto the solid inorganic support and then slow evaporation of the solvent. Another variant is incipient wetness impregnation.[35] In this method, the metal-containing solution (aqueous or organic) is added to a support with a well-defined pore size and then capillary forces drive metal nanoparticles into the pores. Unfortunately, because calcination does not produce a good dispersion, the

gold salts interact only weakly with the support. In addition, the particles suffer from severe agglomeration and side reactions, due to the presence of chloride ions in the support. Gold and chloride ions combine to form bridges, which favors the growth of relatively large particles (>400 nm), making conventional impregnation methods not particularly suitable for catalysis, because the prepared Au NPs are likely inactive. Therefore, an alternative two-step impregnation method was developed for gold supported on Al_2O_3.[36] The gold precursor is adsorbed on Al_2O_3 from an acidified solution and, after washing to remove the excess gold salt, the final solid is treated with a strong base. Following this treatment, no chloride remains in the solid material because it is all converted to an adsorbed hydroxide. Small gold nanoparticles (average diameter of 2.4 nm) prepared in this way showed better catalytical activity.

The double impregnation method is another economically and environmentally friendly alternative for preparation of highly active supported gold nanoparticles. Bowker and co-authors,[37-38] first used this method for preparation of Au NPs supported on TiO_2. The method was later used by other authors, for preparation of Au NPs supported on metal oxides or carbon materials.[34, 39-40]

2.2. Sol-immobilization

The sol-immobilization technique uses colloidal gold prepared by reduction of tetrachloroauric acid by $NaBH_4$, citric acid or other reducing agents, and then deposited on a metal oxides or carbon support.[41] To achieve a good dispersion of the colloidal gold, it can be prepared in solution in the presence of stabilizing ligands such as amines, thiols or a polymer such as polyvinylpyrrolidone.[42-51] The presence of these ligands provides some degree of control over the shape and size of the newly formed nanoparticles. To effectively prepare the heterogenous catalyst and stabilize the formed nanoparticles, an excess of ligands is used. After deposition of colloids on the surface of the inorganic support, the ligands have to be removed, as they can block catalytically active sites of metal nanoparticles.[52] Generally, they can be removed by decomposition at high temperatures (300 °C)[51] or by using of UV light or ozone or by solvothermal treatment.[53] Different types of heterogenous catalyst, for example 1% Au/C, have been prepared using this method.[51]

2.3. Co-precipitation

Co-precipitation is one of the simplest and oldest methods[3] used for the preparation of supported Au NPs and it remains widely used today.[54] This method was first used in 1987 by Haruta's group,[3] by mixing of $HAuCl_4$, sodium carbonate and iron nitrate, leading to the formation of small size gold nanoparticles supported on Fe_2O_3. This prepared catalyst then surprisingly showed catalytic activity for the oxidation of carbon monoxide at a temperature below 0 °C, which had never been described before due to the low affinity of gold for CO absorption at temperatures below 200 °C.[55,56]

2.4. Deposition-precipitation

This method was first used by the Haruta group in 1991.[57] Firstly, a mixture of an insoluble oxide support and $HAuCl_4$ was prepared, followed by the addition of an inorganic base (e.g. NaOH or Na_2CO_3) or urea, which leads to a rapid change in the pH of the solution. This change in the pH value allows the precipitation of target active hydroxide species that are anchored to the surface of the support. The prepared sample is then submitted to a final treatment sequence of washing, filtration and final reduction of Au(III) ions into Au NPs under a flow of H_2. This method led to the preparation of highly dispersed nanoparticles with small sizes (2-3 nm) mainly located at the support surface. Metal oxides may be used as the support, but zeolites and activated carbons are not well tolerated.[58,59] Although if it is a relatively old method for the preparation of supported Au NPs, it is still widely used nowadays.[60-62]

2.5. Liquid-phase reductive deposition

This method, first reported by Sunagawa et al., involves mixing an aqueous solution of $HAuCl_4$ as the gold precursor with NaOH.[63] Later, this procedure also involved the preparation of colloidal gold by the well-described methods of Turkevich-Frens and Brust-Schiffrin.[64] The reductive deposition begins with the adsorption of gold ions onto the surface of the supports where reduction then occurs. The most critical step in this technique is the initial adsorption step. Key factors include precise control of the metal complex precursor through adjustment of the solution conditions. Other factors such as the storage of the suspension until equilibrium is reached and aging under controlled temperature conditions also play an important role. Reductive deposition has also subsequently been used for the preparation of gold nanoparticles supported on other inorganic supports.[65]

2.6. Photochemical deposition

The deposition of metals on semiconductor materials generally occurs via a mechanism involving the reduction of metal ions by conduction band electrons. In some cases, the efficiency of this method can be improved by the use of electron donors such as formaldehyde, methanol, or 2-propanol, which act as continuous sources of electrons upon oxidation. Photodeposition takes place at the photoexcited sites, leading to an enhanced dispersion. Usually, the gold salt is dissolved in a mixture of water, the sacrificial electron donor and the chosen support. Then the mixture is sonicated and irradiated with a UV-lamp with a photodeposition wavelength of 365 nm.[60]

2.7. Ion-exchange

The principle of this method relies on ion exchange between a support and gold ions. This approach is particularly effective for zeolites, but introducing the catalytically active species into the internal cavities of these materials presents certain difficulties. These difficulties mainly arise from the limited availability of suitable cations or cationic complexes capable of accessing the zeolite framework.[66] Still, a wide variety of Au/zeolite systems have been successfully prepared by using this strategy.[67]

Pitchon and co-workers developed a novel method for the synthesis of supported gold catalysts. The method is based on the direct anionic exchange (DAE) between gold species and hydroxyl groups present on the support surface[68, 69] In this approach, an aqueous $HAuCl_4$ solution is added to the support and is heated to 70 °C. The resulting slurry is subsequently filtered, washed with warm water, dried overnight at 120 °C, and calcined under air at 300 °C for 4 h. To ensure complete removal of chloride ions, the dried catalyst is further washed with a concentrated ammonia solution. However, this treatment may pose safety concerns, as the reaction between gold oxide and ammonia can lead to the formation of fulminating gold, a highly explosive compound.[70]

2.8. Ultrasonication

This method is somehow analogous to photodeposition, but the sample is subjected to ultrasonic treatment instead of light irradiation.[71] The procedure was discovered serendipitously during attempts to prepare gold nanoparticles on ZnO via photodeposition. In this study, the ZnO support was synthesized by chemical vapor deposition following a previously reported procedure.[72] The Au/ZnO suspension was left under sonication longer than required, and after this extended sonication period, the mixture exhibited a deep purple coloration, similar to that observed for samples prepared by other deposition methods. After isolation, the resulting material was analyzed by TEM imaging and tested in CO oxidation. It turned out to be the most active catalyst for CO oxidation. Ultrasonication was later used for preparation of Au-NPs supported on Fe_2O_3,[73] MgO,[74] CuO, NiO, La_2O_3, and Y_2O_3.

3. Parameters Influencing the Activity of Gold Nanoparticles

Many different factors influence the catalytic activity of supported gold nanoparticles. These include the particle size and shape, the structure of the surface and presence of oxidized gold atoms, and the interaction between the gold and the support. These factors can be controlled by the type of preparation method and the conditions. The most significant factors are discussed below.

3.1. Size, shape and surface structure of Au NPs

In general, the catalytic activity of Au NPs increases as their size decreases. The reason is twofold: firstly the specific surface area increases as the size decreases. Secondly, and particularly in the case of spherical NPs, the rugosity of the surface increases with decreasing diameter, with terraces, edges and corners, and singularized atoms exhibiting discrete catalytic activity.[75] The influence of all these factors of catalytical activity was investigated in detail by Toshima[76] and was also clearly demonstrated in Haruta's work on low temperature oxidation of CO to CO_2.[3] The influence of gold nanoparticle size on the catalytic dehydrogenation of benzyl alcohol was also studied in oxidative (with O_2) and non-oxidative (without O_2) dehydrogenation reactions.[77] Gold nanoparticles supported on hydrotalcite (Au/HT) with sizes ranging from approximately 2 to 20 nm were synthesized and evaluated. The results obtained demonstrated a strong, size-dependent catalytic activity, with smaller Au nanoparticles exhibiting significantly higher activity, particularly in the non-oxidative reaction. The study showed that low-coordination surface atoms, such as edge and corner atoms, are the most active sites for benzyl alcohol dehydrogenation. In oxidative conditions, oxygen facilitates the reaction, allowing a larger fraction of surface atoms to participate, whereas in non-oxidative conditions the reaction is mainly restricted to edge and corner sites.

Gold and other noble metals tend to form spherical particles, due to the high symmetry of this arrangement of the metal atoms and to minimize the surface area energy. Nanoparticles most commonly exhibit morphologies ranging from quasi-spherical to highly faceted shapes, typically cubic or octahedral. However, small nanoparticles with sizes below 20 nm do not always adopt their equilibrium shape. In this case, multi-twinned nanoparticles (MTPs) with five-fold symmetry are also observed.[78] It is important to note that controlling the morphology of the synthetized Au NPs is not simple. The morphology depends on various factors such as the type of support, presence of defects or impurities.[79]

3.2. Oxidation state of Au NPs

The degree of oxidation of catalytically active gold is even today not well understood. Different types of catalytically active species have been proposed, such as small metallic clusters of Au(0), cationic gold species (Au(I) and/or Au(III)) and anionic gold species.[80-83] The oxidation degree of Au NPs is influenced by many factors, mainly the type of support. The work of Kowalski [84] and his team showed that the oxidation degree of Au NPs changes depending on how the gold is adsorbed on the support. For example, gold atoms adsorbed at a bridge site between the surface oxygen and first-layer titanium ions do not change the oxidation state of titanium (Ti^{4+}). If gold is adsorbed on top of oxygen atoms, charge transfer from metal to surface occurs, leading to the reduction of second-layer titanium ions (Ti^{3+}) and thus to the formation of a positive charge on the gold ($Au^{\delta+}$). In conclusion, the site at which the gold atoms are adsorbed and the nature of the supports are very important for the oxidation degree of Au NPs.[85]

3.3. Interaction with the support

The influence of the support on the catalytic activity of gold nanoparticles is widely described.[33, 86-90] It is known that the support directly affects the electronic structure, stability, and thus catalytic properties of the supported gold nanoparticles. Rather than serving as an inert carrier, the support actively participates in the catalytic process by enabling charge transfer with the gold particles and stabilizing specific oxidation states.[91] Additionally, the nature of the support impacts particle dispersion and resistance to sintering. Strong interactions between the gold and the support also modify the electronic properties of the supported metal. The catalytic active sites are often located at the interface between gold and the support. Reducible oxide supports can supply oxygen and facilitate key reaction steps. In the literature, the influence on the support is mainly discussed for important reactions such as CO oxidation, alcohol oxidation, or the water–gas shift reaction.[91] The literature also shows that the preparation method significantly affects the final performance of the prepared catalyst. On the other hand, dynamic changes under reaction conditions complicate our understanding of the mechanisms. Multiple reaction pathways may coexist depending on the system. Overall, the synergy between the gold nanoparticles and their supports determines catalytic efficiency and selectivity.

4. Characterization of Supported Gold Nanoparticles

The catalytical activity of the supported Au NPs can be influenced by many parameters. Discussions in the literature mainly focus on the effect of the size and shape of the gold particles, the gold oxidation state and interactions with the support.[64] Therefore, methods for in-depth characterization of supported Au NPs are required. A large range of characterization techniques is available to examine and classify these catalysts.[92] Various techniques can be used, depending on which types of characteristics are relevant. For example, techniques such as energy-dispersive X-ray spectroscopy (EDX), X-ray fluorescence (XRF) spectrometry and inductively coupled plasma atomic emission spectroscopy (ICP-AES) are used to determine the elemental composition of the gold catalyst. This is important because other metals, even impurities, can play a role in the catalytic activity. In addition, in the case of bimetallic NPs, synergies in the catalytic activity of the nanoparticles result in high catalytic activity and efficiency.[93] Structural characteristics can be obtained using ultraviolet-visible spectroscopy (UV-Vis), vibrational spectroscopy or neutron diffraction. The shape and the size of gold catalysts can be obtained using scanning electron microscopy (SEM), transmission electron microscopy (TEM), dynamic light scattering (DLS) or variable-angle high-angle annular dark-field (HAADF) imaging down to a certain size. And finally, surface and textural properties of gold catalysts can be provided by techniques based on gas absorption, such as X-ray photoelectron spectroscopy (XPS) or BET surface area analysis. All these techniques can be used separately or in combination to fully characterize the gold catalysts. We present here the most commonly used techniques and examples of the properties they characterize.

4.1. The shape and the size of the gold catalyst

4.1.1. Scanning electron microscopy (SEM) and transmission electron microscopy (TEM). Scanning electron microscopy (SEM) and transmission electron microscopy (TEM) are microscopic techniques which are used for high-resolution imaging.[94] Both provide information about the shape and size of gold nanoparticles, as well as information about the support (e.g., structure, including pores and their size). The SEM and TEM techniques are based on the interaction between an electron beam with a constant density electron flow and the sample under vacuum. When the electron beam reaches the sample, some of the electrons are transmitted and some are

scattered. How electrons interact with sample depends on many factors such as the density and size of the sample or its elemental composition.

The difference between the two techniques is based on the range of the electron energies in the beam. In the case of TEM, the range 80 - 300 keV is used and in the case of SEM, a lower range is used, typically 1-30 keV. The method selected is related to the target application. TEM is mainly used for deeper analysis of a sample, because it provides information not only about the size and shape of the nanoparticles, but also an accurate estimation of the nanoparticle homogeneity.[92] The SEM, on the other hand, is used to examine the surface. In this case, electrons from the electron beam interact with sample and produce back-scattered electrons, secondary electrons and characteristic X-rays.[94] All these signals are collected and provide a final image of the sample with resolution between 1-20 nm.

4.1.2. Dynamic light scattering (DLS). This technique is widely used for characterization of supported Au NPs. It is mainly used for the determination of the size of the nanoparticles, but it is also suitable for the evaluation of the shape and surface modifications.[92, 95] The method is based on the measurement of the hydrodynamic size of particles and therefore it is performed only for particles in colloidal suspension. This measurement also includes the physical size of the nanoparticle core, the surface coating and the solvent layer associated with the particle. The suspension is illuminated with a laser beam, and the light is scattered by the particles. Due to the Brownian motion of the particles, the intensity of the scattered light fluctuates over time. Analysis of these intensity fluctuations provides information about diffusion processes, allowing the calculation of the particle size using the Stokes–Einstein equation. Dynamic light scattering has many advantages, but one of the main limitations of this method is that large particles scatter much more light than small particles and even a small number of large particles can mask the contribution of smaller particles.

4.1.3. X-Ray diffraction (XRD). This non-destructive technique provides information about the crystalline structure of the gold nanoparticles,[92, 95] the grain size, the lattice parameters and possibly also information about the support. It is based on Bragg's law and exploits the wave nature of X-rays and their interaction with a sample surface. The size of the gold nanoparticles can be obtained from the Scherrer equation,[96] using the Full Width at Half Maximum (FWHM) of the most intense peak in the diffraction pattern. Values for the nanoparticle size thus obtained are generally in very good agreement with values obtained by TEM technique. Unfortunately, due to the low intensity of the diffraction peaks during XRD measurements, this technique cannot be used for nanoparticle sizes below 2 nm or where the metal loading is below 0.5 wt %.

4.2. The surface and textural properties of the gold catalyst

4.2.1. X-ray photoelectron spectroscopy (XPS). One of the most widely used techniques for characterization of nanoparticles is X-ray photoelectron spectroscopy (XPS). This technique provides a detailed characterization of the electronic structure, elemental composition, and oxidation state of the elements present on the surface of the analyzed sample. The technique is based on the photoelectric effect, a physical phenomenon arising from the interaction between radiation and matter and characterized by the emission of electrons from the surface of the metal with a characteristic wavelength.

For nanoparticles with a core-shell structure, a slightly different approach is required. In this case, the major problem is interpreting the XPS data, which requires knowledge of the chemical core and the size of the nanoparticles. A key challenge is converting the relative XPS intensities, which are usually expressed as a ratio of the intensity of photoelectrons from the shell to the intensity of photoelectrons from the core, into shell thicknesses. Shard published an empirical method to convert XPS intensities into shell thicknesses for spherical core-shell metal nanoparticles.[97] X-Ray photoelectron spectroscopy can be also used to detect the oxidation state of Au NPs supported on CeO_2, TiO_2 and SiO_2 synthetized by the deposition precipitation method.[98,99] After

measurement, XPS curves are obtained, showing the specific binding energy, which corresponds to the different contribution of the gold species. For example, a band at about 84 eV is typically attributed to Au(0), the peak around 85 eV is attributed to Au(I) species and the peak around 86 eV corresponds to the Au(III) species.[99]

4.2.2. BET surface area analysis. The BET surface area analysis is a useful calculation method to determine the surface area based on N_2 adsorption.[100] This method is similar to the Langmuir theory of absorption, which explains adsorption by assuming an adsorbate behaves as an ideal gas at isothermal conditions. According to the model, adsorption and desorption are reversible processes. BET surface area analysis also considers multilayered gas molecule adsorption, which does not require completion of one layer before the formation of the next layer begins.[101] Unfortunately, the BET method does not make it possible to differentiate between the catalytically active species and the support. Consequently, the metal dispersion, specific surface area of the active phase, and the particle size of the supported metal nanoparticles are typically evaluated by chemisorption techniques employing H_2, CO, or O_2 as probe molecules.[102-104] Therefore, this method is highly limited by the properties of the support and cannot be used generally.

4.3. The elemental composition of the gold catalyst

4.3.1. X-ray spectroscopy (EDX). This is a spectroscopic technique used for elemental analysis of solid samples. It detects the characteristic X-rays emitted by atoms when they are stimulated by an electron beam, typically in a scanning electron microscope (SEM) or transmission electron microscope (TEM). It is mainly used to identify which elements are present in the sample, determine their relative amounts and map the spatial distribution of atoms, in this case gold atoms, within the material using elemental maps in STEM-EDX.

Modern TEM-STEM machines are combined with large solid-angle EDX detectors that can even identify individual metal atoms or single-atom catalysts, though this requires advanced instrumentation and careful interpretation.[89, 105] This technique provides essential data on composition, but these are unfortunately rarely sufficient on their own for a complete characterization of the catalyst. This method therefore has to be combined with other spectroscopic methods.

4.3.2. X-ray fluorescence (XRF) spectrometry. The X-ray fluorescence spectrometry (XRF) is, like EDX, a non-destructive analytical technique. It is widely used in materials science, geology, environmental analysis, and catalyst characterization, mainly to determine the elemental composition of a sample. For the analysis of metal-based solid catalysts, it is primarily used for elemental identification, e.g., the presence of a metal, but it cannot be used to determine the oxidation state. It is very useful method for determining the total metal content on supported catalysts (e.g., Au/TiO_2, Au/Al_2O_3) before and after the catalytic reaction. However, like the previous method, XRF is often used in combination with TEM/SEM, XPS, ICP-OES or ICP-MS techniques. [89, 105]

4.3.3. Inductively coupled plasma atomic emission spectroscopy (ICP-AES). This is a sophisticated analytical method used to measure and identify the elemental composition of materials. ICP-AES is well-known for its excellent accuracy, sensitivity and capacity for instant analysis of multiple elements in a sample. The method is based on the principle of atomic emission spectrometry, in which atoms and ions in an analyzed sample are driven to higher energy states using an inductively coupled plasma (ICP). Then, irradiated atoms release light at specific wavelengths when they return to their ground state. Measured wavelengths correlate directly with the element's concentration in the sample.

This method is generally used determine if there is leaching of gold species from Au NPs,[106] but it can also be used to measure the Au loading on metal-oxide supports (TiO_2, ZrO_2 or CeO_2).[107, 108]

While this method has many benefits, including excellent sensitivity, quick analysis time and multi-element capabilities, it also has drawbacks, such as complex sample preparation and machine calibration requirements.

5. Supported Gold Nanoparticles in the Multistep Synthesis of Valuable Chemicals

Multistep catalytic reactions have attracted extensive interest because of their ability to reduce reaction steps, energy consumption, and waste. These types of reactions are designed for the synthesis of complex molecules in one operation from simple starting materials. Different terminology, such as one-pot, tandem, cascade, sequential or domino reaction, is used, depending on whether the reaction is inter- or intramolecular (Figure 1.).

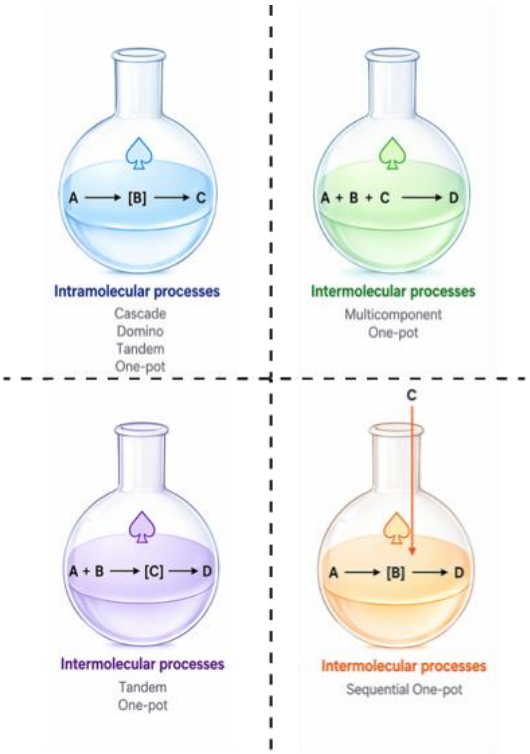

Figure 1. Examples of terminology for multistep catalytic reactions.

However, producing highly efficient multicatalytic systems remains very challenging. The main reasons are the difficulty of integrating multiple active catalytic sites into one reaction and incompatibility of the different reaction conditions.

5.1. Supported Au NPs in the multistep synthesis

5.1.1. Synthesis of oxygen-containing compounds. Oxygen-containing heterocycles are considered as very valuable compounds, and they are widely found in natural products, pharmaceuticals, agrochemicals or compounds with olfactory properties.[109]

Sophisticated oxygen-containing heterocycles can be prepared in a one-pot/2 steps sequence using ultrasmall gold nanoparticles via 1,6-enyne cyclodimerization followed by Diels-Alder cycloaddition.[85] The study reports the design, synthesis, and catalytic evaluation of gold nanoparticles (< 2 nm) enclosed in the rigid networks of polymantane ligands (diamondoids). Gold nanoparticles were synthesized in one step using ditopic diamondoids (e.g., bisadamantane or diamantane dithiols) which served as bulky stabilizers and linkers to build

dense networks. The material was further oxidized and described as providing Au^+ ions at the surface, stabilized by sulfinate ions generated simultaneously upon sulphur oxidation, and acting as the active species. The authors showed high selectivity in enyne cycloisomerization, transforming dimethyl allyl(propargyl)malonate into a 5-membered conjugated diene with excellent regiocontrol (Scheme 1).[85] Under homogeneous conditions, this cyclization gives various mixtures of five- and six-membered dienes **2** and **3**. In the next step, the cycloisomerization product underwent the Diels–Alder reaction with maleic anhydride (Scheme 1). The reaction proceeded smoothly and the Diels-Alder product **4** was isolated in quantitative yield. This method illustrates the high potential of supported Au NPs for multistep transformations leading to valuable compounds.

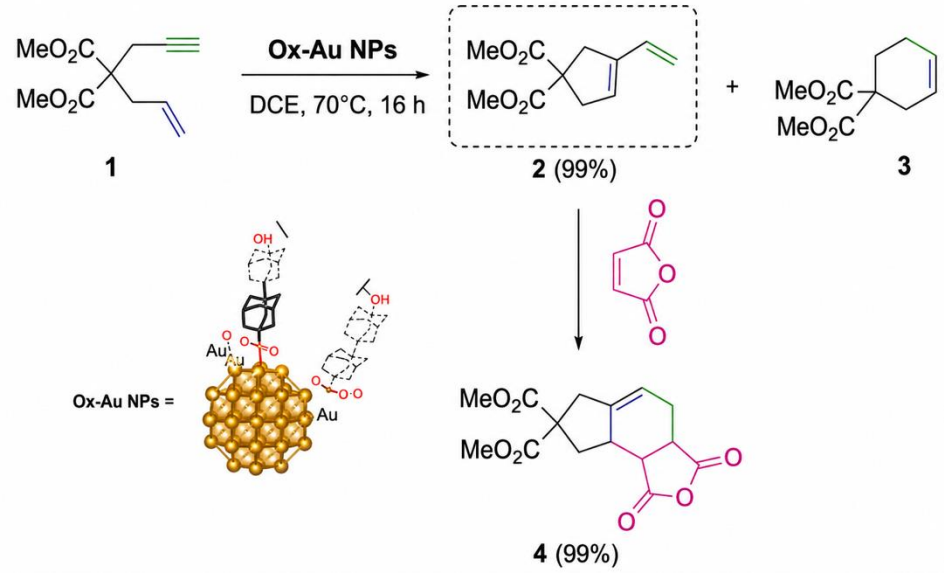

Scheme 1. Cycloisomerization of dimethylallyl(propargyl)malonate **1** using oxidized Au NPs and cascade Diels–Alder reaction.

A large portion of our research focuses on using of supported metal catalysts, including Au NPs, for tandem reactions. Originally, the generation of carbonyl function by oxidation reaction was investigated.[12] This newly formed carbonyl function provides a new electrophilic center, capable of initiating cascade sequences. This approach was used for example in the synthesis of (±)-*ortho*-tetrahydrocannabinol (THC) isomers and analogues by using simple, naturally occurring alcohols.[110] The tandem sequence involved an oxidation/double cyclization/Friedel-Crafts aldol arylation catalyzed by Au NPs/Al_2O_3 and Ti-MMT (Ti(IV)-doped montmorillonite). The reaction sequence was performed in two steps in batch mode or as single operation in a continuous-flow reactor (Scheme 2).

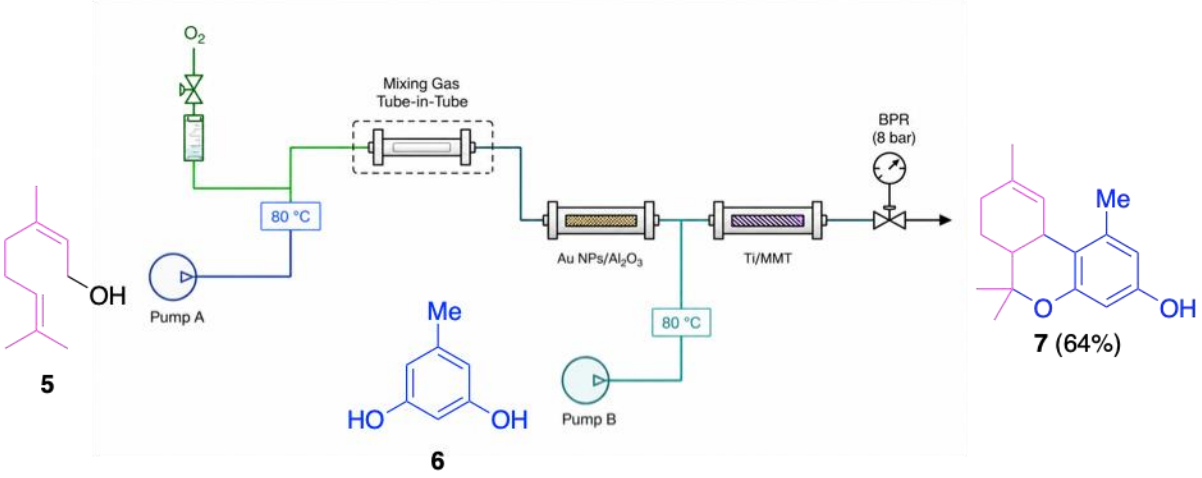

Scheme 2. Synthesis of *ortho*-THCs by using of continuous-flow setup (TBHP: tert-butyl hydroperoxide, BPR: back-pressure regulator).

A sequential one-pot oxidation/hetero-Michael addition/aldolization/crotonization was then developed by combining supported Au NPs and base-catalysis under an O_2 atmosphere. Benzylic and allylic alcohols derivatives were condensed with salicylaldehydes en route to substituted *2H*-chromenes.[111] The reaction can also be applied to substituted quinolines synthesis using *ortho*-aminobenzaldehyde. Interestingly, *ortho*-aminobenzyl alcohol can be used as starting material together with an allylic alcohol, and both can be oxidized to their corresponding carbonyl compound in the sequence leading to quinolines via a one pot/5-step sequence (Scheme 3).

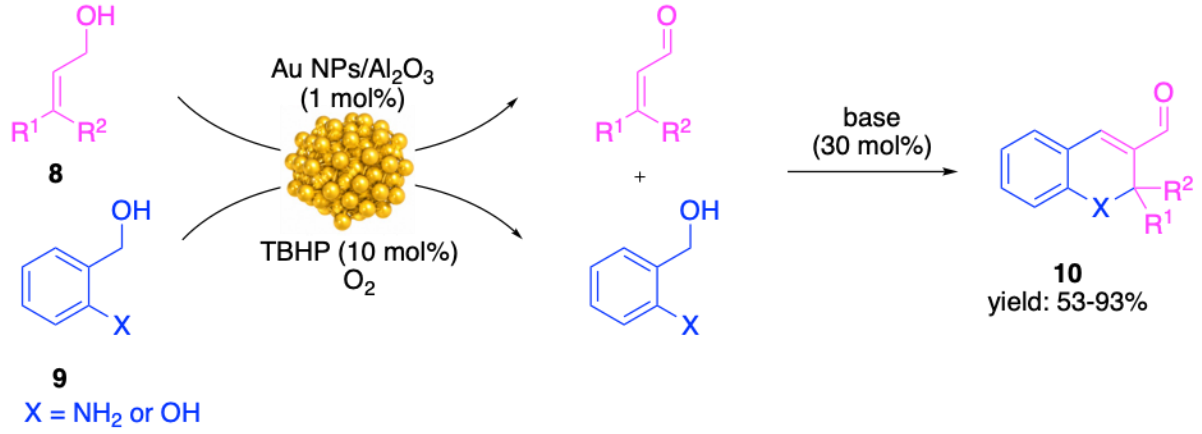

Scheme 3. Sequential one-pot synthesis of *2H*-chromene and quinoline derivatives catalyzed by Au NPs and organic or mineral bases.

Targeting other types of chromenes, commercially available gold nanoparticles supported on TiO_2 (Au NPs/TiO_2) have been used as an efficient catalyst in tandem cyclization/reduction and cyclization/hydroalkoxylation reactions (Scheme 4).[112]

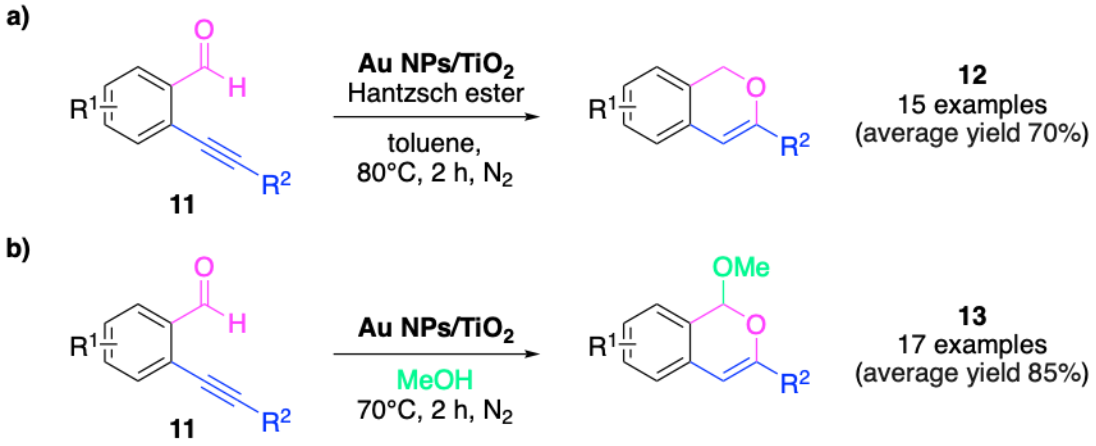

Scheme 4. Au NPs/TiO_2 catalytic system for tandem cyclisation/reduction or cyclisation/hydroalkoxylation.

Derivatives of *ortho*-alkynyl benzaldehyde were used as starting materials for both transformations. In the case of the tandem cyclization/reduction catalytic system of Au NPs/TiO_2 in the presence of Hantzsch ester, 15 examples were reported with an average yield of 70% (Scheme 3a). For tandem cyclization/hydroalkoxylation, the same catalytic system was used, but Hantzsch ester was replaced with MeOH as the nucleophile. With this tandem reaction 17 examples of 1*H*-isochromene derivatives were isolated in average yield of 85% (Scheme 3b). Notably, the reaction proceeded smoothly and led to formation of target compounds in an exclusively 6-*endo* selective manner, which was not always fully achieved in the case of homogenous catalysis.[113] In addition, the tandem cyclization/hydroalkoxylation was also performed in a continuous flow reactor, scaling up the reaction by a factor of 10 without loss of efficiency. The developed method was then successfully applied as a key step in the total synthesis of a biologically active isochromene derivative.

Supported Au NPs have also been used for the oxidative valorization of biomass-derived furfural **14** with aliphatic alcohols.[114] This work reported the design, synthesis and characterization of Au@UiO-66-X catalysts, where UiO-66 is a Zr-based MOF functionalized with a hydrogen atom or different functional groups (X = H, NH_2, NO_2, COOH). Prepared catalysts were then tested in the oxidative transformation of furfural with methanol and ethanol under an O_2 atmosphere (Scheme 5). In the furfural–methanol–O_2 system, the catalyst promoted oxidative esterification, converting furfural into methyl-2-furoate (**15**) with full conversion of the starting material and very high selectivity (Scheme 5 - Path A). On the other hand, when ethanol was used as the alcohol, another reaction pathway emerged. The catalyst favored an oxidative condensation reaction to form vinylogous products, such as furan-2-acrolein (**16**), through an aldol-type coupling reaction between in-situ generated acetaldehyde and furfural (Scheme 5 - Path B).

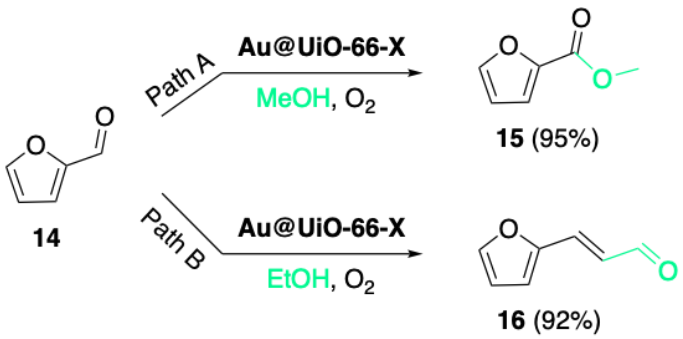

Scheme 5. Oxidation transformation of furfural **14** with methanol or ethanol catalyzed by Au@UiO-66.

A tunable heterogeneous catalytic system that can selectively valorize furfural, a key biomass molecule, into valuable chemicals via oxidative esterification and oxidative condensation pathways using only O_2 as the oxidant was thus demonstrated.

Supported Au nanoparticles on TiO_2 efficiently catalyze the tandem conversion of skipped diynones into γ-pyrones or *N*-methyl-4-pyridones, depending on the nucleophile employed.[115] In aqueous dioxane, water initiates a hydration/6-*endo*-dig cyclization sequence to furnish *γ*-pyrones. Replacing water with aqueous methylamine switches the reaction pathway to hydroamination followed by Au-catalyzed 6-*endo* cyclization, leading to formation of *N*-methyl-4-pyridones in good yields (69–79%). We note that, unlike homogeneous Au(I) catalysts, the heterogeneous Au/TiO_2 catalyst completely suppresses the competing 5-*exo* cyclization, that would lead to 3(2*H*)-furanones, and thus exhibits excellent regioselectivity.

5.1.2 Synthesis of nitrogen containing compounds. The amide function constitutes an essential class of functional groups, and amide compounds have been the focus of intensive research in the development of synthetic methods in organic chemistry. The amide bond is a key structural motif in the construction of complex organic molecules, frameworks and polymers, and peptide bonds in particular play an essential role in biological systems. Many different approaches can be used to synthesize amides. Kobayashi described an elegant and effective heterogeneous catalytic strategy to prepare amides by using simple alcohols and amines in the presence of molecular oxygen as the oxidant (Scheme 6a).[116] This work describes the preparation of heterogeneous-polymer-incarcerated bimetallic Au/M nanoparticles (PICB-Au/M) and their use in the synthesis of amides by oxidative amination of alcohols.

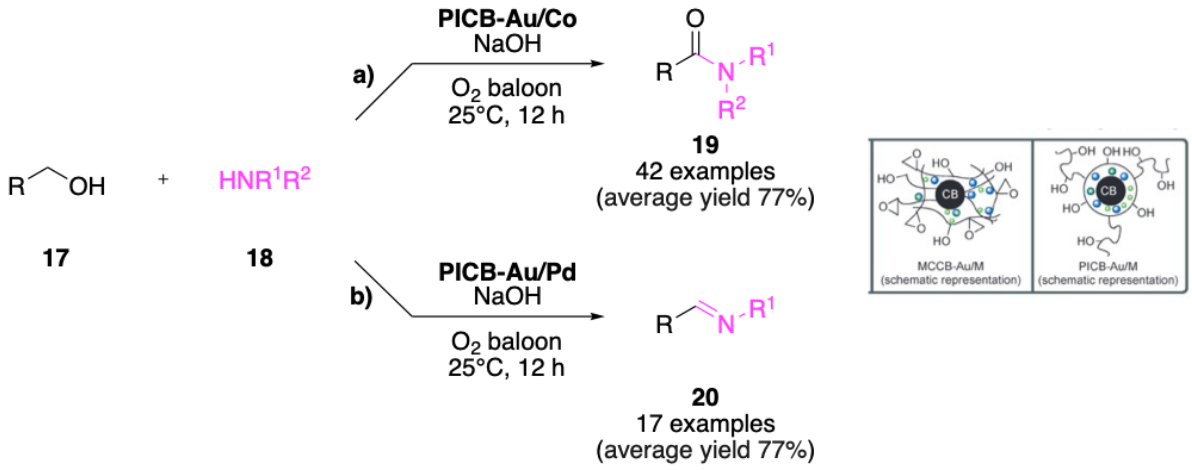

Scheme 6. Synthesis of amides and imines *via* tandem oxidative amination of alcohols.

The process involves a tandem oxidation of the alcohol to the corresponding aldehyde, which consequently reacts with an amine in a one-pot fashion. The reaction allowed a large scope of substrates such as activated alcohols to be efficiently converted (e.g., benzylic, allylic, propargylic), but it was also successfully applied on nonactivated aliphatic alcohols leading to synthesis of 42 different amides. A significant advantage over other amide synthesis methods is that the only by-product is water and the catalyst can very easily be recycled, making this method highly green and sustainable.

The same research team also reported a heterogeneous catalytic method for the direct aerobic oxidative coupling of alcohols and amines to imines using carbon-incarcerated gold/palladium (Au/Pd) alloy nanoparticles (PICB-Au/Pd) and molecular oxygen (O_2) as the oxidant (Scheme 6b).[117] Again, the reaction tolerated a large substrate scope and this method made it possible to selectively prepare 17 imines with yields in the range 58 – 95%.

Fang and Zhao published an improved method of synthesis of imines using Au NPs supported on Zn-doped Al_2O_3 under O_2 atmosphere without additive.[118] The catalyst exhibited high activity and selectivity under mild conditions, offering a greener alternative to traditional imine synthesis. Varying the amount of Zn^{2+} dopant and the calcination temperature of the alumina support was crucial to tune the catalyst's performance by affecting the active oxygen species on the surface and the acid–base properties and thus influencing the alcohol oxidation, which is the rate-determining step. The catalyst showed a good stability and recyclability, maintaining the activity over multiple runs and was effective also at the gram-scale.

The first synthesis of a nanostructured multifunctional catalyst was described in 2020 by Huang and Cao.[119] The catalyst consisted of an imidazolium-based cationic covalent triazine frameworks (ICTF) host with Au NPs guest (Au@ICTF). It was used in a tandem deacetalisation-Knoevenagel condensation-reduction reaction and showed excellent catalytic activity and selectivity.

In the process, the ICTFs exhibiting Lewis acid sites promoted the deacetalization reaction, while free chloride anions and triazinic *N* species played the role of Lewis base sites and catalyzed the Knoevenagel condensation reaction. The physical segregation of both Lewis acids and bases was key here in the success of the process avoiding self-quenching of the catalysts. In the last step, Au NPs acted as a hydrogenation catalyst to selectively reduce the ester function and the carbon-carbon double bond to afford the polysubstituted arylamines containing a b-cyanohydrin motif.

An efficient and sustainable approach to valuable *N*-heterocycles were described by using of the oxidative cyclization of conjugated allenones with alkynylamines catalyzed by supported gold nanoparticles.[120] Reaction leaded to the synthesis of 3-keto pyridines. The supported Au NPs catalyst enabled the selective construction of the pyridine core under mild oxidative conditions while exhibiting broad substrate scope and good functional group tolerance. The methodology represents an attractive alternative to conventional homogeneous gold catalysis, combining high catalytic efficiency with the practical advantages of catalyst recovery and recyclability.

5.2. Supported Au NPs-enzyme hybrids in the multistep synthesis.

As an alternative to classical supported Au NPs catalysis for tandem reactions, nanoparticles were combined with enzymes to produce chemoenzymatic cascade reactions. This type of hybrid material showed a dual catalytic activity, namely enzymatic and metal-mediated. The design, synthesis and catalytic evaluation of novel hybrid catalysts composed of Ag or Au NPs integrated with lipase or enzyme–polymer conjugates in aqueous media at room temperature has been reported (Scheme 7).[121] Lipase B from *Candida antarctica* (CALB) or enzyme–polymer conjugates served as biotemplates and stabilizing scaffolds for the nanoparticles. The

structure and size of the nanobiohybrids varied significantly depending on pH and the nature of the protein or bioconjugate used.

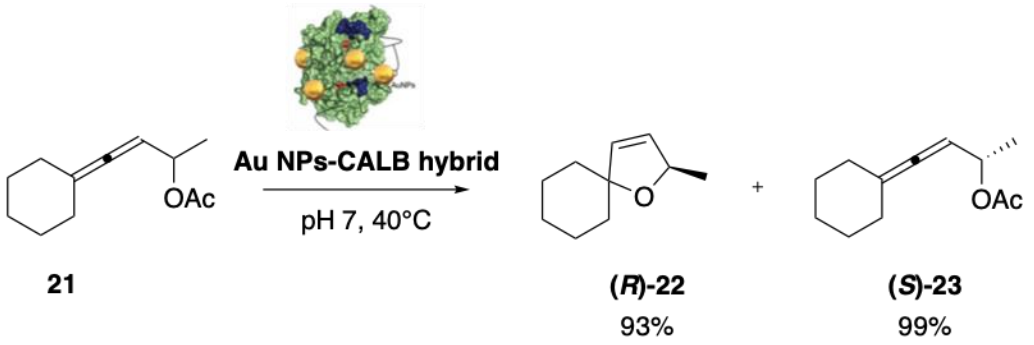

Scheme 7. Synthesis of enantioenriched *O*-heterocycles *via* Au NP–enzyme–polymer hybrids.

Au NPs or Au NPs–enzyme–polymer hybrids efficiently converted allenic substrates **21** into enantioenriched *O*-heterocycles with high stereoselectivity by merging lipase-catalyzed kinetic resolution with metal-catalyzed cyclization. This approach opens new opportunities for developing other one-pot chemoenzymatic cascade reactions and illustrates how protein–polymer scaffolds can control nanoparticle formation.

Another interesting group of supported gold nanoparticles used for tandem reactions are nanozymes, which are nanoparticles (NPs) that exhibit enzyme-like properties. Generally, they overcome the drawbacks of natural enzymes, such as easy deactivation, high cost, or poor recyclability, and they thus constitue highly promising alternatives. This concept of artifical nanozyme was used in cascade reactions of involving glucose-oxidative phosphorylation.[122] Silica microspheres containing encapsulated gold nanoparticles acted as nanozymes which catalyzed two enzymatic-like steps: (*i*) the oxidation of glucose to gluconic acid and (*ii*) the reduction of oxygen. The final catalytic cascade reaction produced a proton gradient across the microsphere membrane that drove natural ATP synthase, reconstituted on the surface, to synthesize ATP from ADP and inorganic phosphate.

The hybrid assembly exhibited a high activity for oxidative phosphorylation, approaching the efficiency of cellular mitochondria, and thus provided a prototype for bioenergy conversion systems that integrate artificial catalysts with biological machinery.

In another study, a glucose oxidase (GOD)-like catalytic mechanism with different noble metal nanozymes was reported, providing fundamental insights into how metal nanoparticles mimic enzymatic glucose oxidation.[123] The authors performed a study of Au, Pt, Pd, Ru, Rh, and Ir nanoparticles as oxidants and demonstrated that glucose oxidation proceeds through a two-step mechanism involving : (*i*) glucose dehydrogenation on the metal surface and (*ii*) oxygen reduction. Notably, Au NPs behaved similarly to the GOD-like catalyzed pathway by catalyzing the two-electron reduction of O_2 to H_2O_2, whereas other noble metals, such as platinum, palladium, ruthenium, rhodium, and iridium preferentially reduced O_2 to H_2O *via* multi-electron pathways.

It is also well known that “naked” Au NPs, without protective ligands or supports of any kind, have glucose oxidase- and peroxidase-like activity, but their activities occur at different optimal pH values. On the other hand, “non-naked” Au NPs, prepared by using of a protein as a protective agent, show dual enzyme-like activity at the same pH, enabling a catalytic cascade (i.e., oxidation followed by a second transformation) in one

pot.[124] It is worth noting that the protein as the protector not only stabilizes the GOD-like function, but also allows further surface modification without loss of the catalytical activity.

A similar study based on the use of biogenic gold nanoparticles to produce a multienzyme cascade reaction was published.[125]

The Au NPs act as an artificial enzymes, which are capable of catalyzing a cascade reaction analogous to an enzyme system. Firstly, glucose is oxidized to generate gluconic acid and hydrogen peroxide (H_2O_2), mimicking glucose oxidase activity. In the next step, hydrogen peroxide is used, and nanoparticles oxidize chromogenic substrates such as 3,3′,5,5′-tetramethylbenzidine (TMB), mimicking a peroxidase-like activity.

All publications dealing with the usie of nanozymes demonstrate its high potential for applications in biosensing, immunoassays and medical diagnostics.

5.3. Bimetallic Au NPs in the multistep synthesis

The first direct olefination of alcohols through a tandem one-pot oxidation followed by HWE reaction using heterogeneous bimetallic Au/Pd NPs as the catalyst was described by Kobayashi.[126] In this work, heterogenous nanoparticles were used effectively in a multistep cascade reaction combining an oxidation step and a C-C bond formation to achieve a one-pot stereoselective synthesis under aqueous and aerobic conditions. The system integrates the individual steps of a synthetic sequence, each catalyzed by a tailored metal nanoparticle. The robust nanocomposite PI/CB-Au/Pd catalyst (PI/CB = polymer incarcerated carbon black) was used in a tandem aerobic oxidation–HWE reaction (Scheme 8). A large scope of substrates were tested, including benzyl alcohols substituted with electron-withdrawing and electron-donating groups, heteroaryl-substituted alcohols and aliphatic alcohols. The desired products were isolated in yields of 58–83% yields with excellent selectivity. Then a tandem process was added to the sequence, featuring an asymmetric 1,4-addition reaction catalyzed by chiral Rh nanoparticles. The final product was isolated in high yield and enantioselectivity (93–99% ee). Crucially, no intermediates had to be isolated during this tandem process and that the catalyst could be recycled without loss of activity.

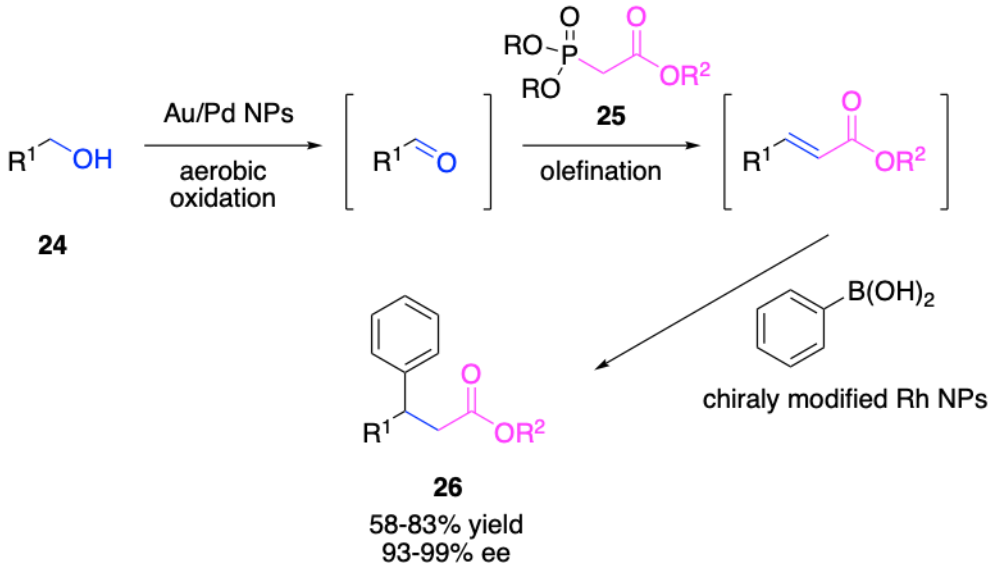

Scheme 8. Sequential alcohol oxidation, olefination, and asymmetric 1,4-addition reaction catalyzed by Au/Pd NPs and Rh NPs.

The electrochemical reduction of carbon dioxide (CO_2) into multi-carbon liquid products, for example ethanol or n-propanol, is a major research direction in renewable energy conversion and storage. Traditionaly, Cu catalysts are used for this transformation but they suffer from limited selectivity. This problem was resolved using Au NPs deposited onto polycrystalline Cu foil, which led to the formation of a bimetallic Au/Cu composite electrode.[127] Under electrochemical CO_2 reduction conditions, Au NPs acted as a highly active catalyst for CO generation at low overpotentials and the locally high CO flux then fed adjacent Cu sites where further reduction and C–C coupling occured. This tandem process increased the local intermediate (*CO) concentration on Cu, facilitating deeper reduction to alcohols with longer carbon chains. This electrocatalytic strategy offers a pathway to improved selectivity and efficiency in producing higher-value liquid fuels from CO_2.

The Suzuki cross-coupling reaction is one of the most useful tools for the formation of C–C bonds and it plays significant role in organic synthesis. This reaction often requires very often elevated temperatures and additional stoichiometric reagents, however. A greener and sustainable alternative has been reported using solar energy to efficiently achieve the desired transformation (Scheme 9). A visible-light-induced photocatalytic Suzuki cross-coupling reaction was thus reported by using AuPd alloy NPs supported on spherical SiO_2.[128] Various arylhalides and phenylboronic acids were used, demonstrating that this method is applicable to a wide range of substrates. More than 15 examples of Suzuki cross-coupling reaction products were isolated in moderate to excellent yields (48-91%) with high selectivities (> 98%).

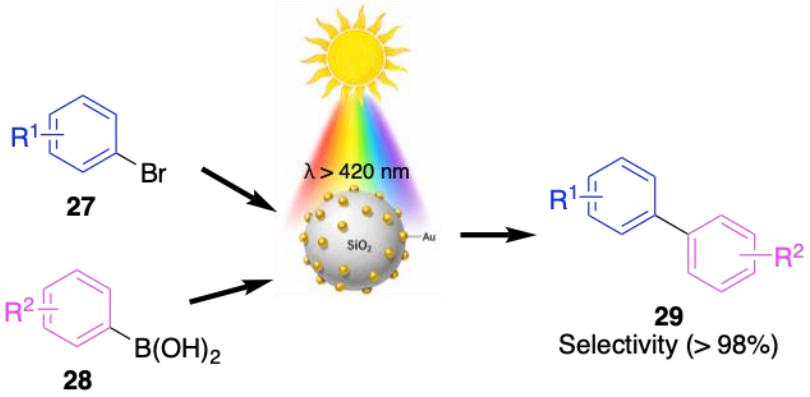

Scheme 9. Photocatalyzed Suzuki cross-coupling reaction catalysed by AuPd NPs/SiO_2.

This work was conceptually distinct from conventional strategies that tune the optical absorption properties of plasmonic Au or AuPd nanoparticles through variations in particle size and morphology, introducing an alternative approach based on a near-field scattering–promoted optical absorption model.
This strategy can be further extended to manipulate and enhance the light-harvesting capability of AuPd alloy nanoparticles, as well as other bimetallic systems, thereby improving the efficiency of photo-driven Suzuki cross-coupling and related C–C bond-forming reactions for the synthesis of high value-added chemicals.

Conclusions

Supported gold nanoparticles have emerged as a versatile and highly promising class of catalytic materials, demonstrating unique physicochemical properties. This review has focused on the synthesis of supported Au nanoparticles, highlighting the importance of preparation methods, support selection, and control over particle

size, morphology and metal–support interactions. These parameters are critical in tailoring catalytic performance, stability, and selectivity.

The application of supported gold nanoparticles in the synthesis of fine chemicals has demonstrated their remarkable potential in promoting cascade and tandem reactions, reducing the need for intermediate purification steps and enhancing overall process efficiency through both atom- and step-economy approaches. Their ability to facilitate selective oxidation, reduction, and carbon–carbon bond-forming reactions under mild conditions makes them especially attractive for the sustainable production of high-value chemicals.

Despite these advances, several challenges remain. These include improving catalyst durability, achieving precise control of active site structure, and scaling up synthesis methods while maintaining reproducibility and cost-effectiveness. Furthermore, a more comprehensive understanding of reaction mechanisms is still needed though operando analysis as well as state-of-the-art microscopy techniques, improving both magnification and resolution. Anticipation of catalytic properties at the surface remains complex besides elementary steps such as hydrogen/oxygen adsorption already widely used in redox processes. The strategy of discovery of novel reactivities in homogeneous conditions followed by transfer to heterogeneous conditions remains thus relevant, practical and scalable.

Future research should focus on expanding the scope of the reactions and exploring synergistic effects in bimetallic or multifunctional systems. Considering the number of variables, the number of optimization steps, and the lack of deep mechanistic understanding of surface reactivities, optimum localisation by using AI techniques such as machine learning could fasten catalysts and conditions identification.

In conclusion, supported gold nanoparticles represent a powerful platform for advancing green and efficient multistep synthesis strategies, with ever-increasing cost for gold materials thus requiring relevant immobilization and recycling approaches. Continued interdisciplinary efforts will be essential to fully realize their potential in both academic and industrial applications.

Acknowledgements

This work was supported by Université Côte d'Azur and CNRS, and by the French government through the France 2030 investment plan managed by the National Research Agency (ANR), as part of the Initiative of Excellence of Université Côte d'Azur under reference number ANR-15-IDEX-01. We are grateful to the Université Côte d'Azur Office of International Scientific Visibility for English language editing of the manuscript.

References

1. Gerke, R.H.; Rourke, M.D. *J. Am. Chem. Soc.* **1927**, *49*, 1855. https://doi.org/10.1021/ja01407a001
2. Bond, G.C.; Sermon, P.A. *Gold Bull.* **1973**, *6*, 102. https://doi.org/10.1007/BF03215018
3. Haruta, M.; Kobayashi, T.; Sano, H.; Yamada, N. *Chem. Lett.* **1987**, *16*, 405. https://doi.org/10.1246/cl.1987.405
4. Nkosi, B.; Coville, N.J.; Hutchings, G.J. *J. Chem. Soc. Chem. Commun.* **1988**, 71. https://doi.org/10.1039/C39880000071

5. Prati, L.; Rossi, M. *J. Catal.***1988**, *176*, 552. https://doi.org/10.1006/jcat.1998.2078
6. Edwards, J.K.; Solsona, B.E.; Landon, P.; Carley, A.F.; Herzing, A.; Kiely, C.J.; Hutchings, G.J. *J. Catal.* **2005**, *236*, 69. https://doi.org/10.1016/j.jcat.2005.09.015
7. Della Pina, C.; Falletta, E.; Prati, L.; Rossi, M. *Chem. Soc. Rev.* **2008**, *37*, 2077. https://doi.org/10.1039/B707319B
8. Gutiérrez, L.-F.; Hamoudi, S.; Belkacemi, K. *Appl. Catal. A Gen.* **2011**, *402*, 94. https://doi.org/10.1016/j.apcata.2012.03.025
9. Centeno, M.; Ramírez Reina, T.; Ivanova, S.; Laguna, O.; Odriozola, *Catalysts* **2016**, *6*, 158. https://doi.org/10.1016/j.apcata.2012.03.025
10. Saavedra, J.; Pursell, C.J.; Chandler, B.D. *J. Am. Chem. Soc.* **2018**, *140*, 3712. https://doi.org/10.1021/jacs.7b12758
11. Megías-Sayago, C.; Santos, J.L.; Ammari, F.; Chenouf, M.; Odriozola, J.A. *Catal. Today* **2018**, *306*, 183. https://doi.org/10.1016/j.cattod.2017.01.007
12. Hutchings, G.J. *ACS Cent. Sci.* **2018**, *4*, 1095. https://doi.org/10.1021/acscentsci.8b00306
13. Claus, P. *Appl. Catal. A Gen.* **2005**, *291*, 222. https://doi.org/10.1016/j.apcata.2004.12.048
14. Peng, S.; Sun, X.; Sun, L.; Zhang, M.; Zheng, Y.; Su, H.; Qi, C. *Catal. Lett.* **2019**, *149*, 465. https://doi.org/10.1007/s10562-018-2628-5
15. Fu, Q.; Weber, A.; Flytzani-Stephanopoulos, M. *Catal. Lett.* **2001**, *77*, 87. https://doi.org/10.1023/A:1012666128812
16. Flytzani-Stephanopoulos, M.; Fu, Q.; Saltsburg, H. *Science* **2003**, *301*, 935–938. https://doi.org/10.1126/science.108572
17. Barakat, T.; Rooke, J.C.; Genty, E.; Cousin, R.; Siffert, S.; Su, B.-L. *Energy Environ. Sci.* **2013**, *6*, 371. https://doi.org/10.1039/C2EE22859A
18. Conte, M.; Carley, A.F.; Heirene, C.; Willock, D.J.; Johnston, P.; Herzing, A.A.; Kiely, C.J.; Hutchings, G.J. *J. Catal.***2007**, *250*, 231–239. https://doi.org/10.1016/j.jcat.2007.06.018
19. Nkosi, B.; Coville, N.J.; Hutchings, G.J.; Adams, M.D.; Friedl, J.; Wagner, F.E. *J. Catal.* **1991**, *128*, 366. https://doi.org/10.1016/0021-9517(91)90295-F
20. Akram, M.O.; Banerjee, S.; Saswade, S.S.; Bedi, V.; Patil, N.T. *Chem. Commun.* **2018**, *54*, 11069. https://doi.org/10.1039/C8CC05601C
21. Carrettin, S.; Guzman, J.; Corma, A. *Angew. Chem. Int. Ed.* **2005**, *44*, 2242. https://doi.org/10.1002/anie.200462560
22. Gorodetskii, V.; Lauterbach, J.; Rotermund, H.H.; Block, J.H.; Ertl, G. *Nature* **1994**, *370*, 276. https://doi.org/10.1038/370276a0
23. Nguyen, L.Q.; Salim, C.; Hinode, H. *Appl. Catal. B Environ.* **2010**, *96*, 299. https://doi.org/10.1016/j.apcatb.2010.02.020
24. Ueda, A.; Oshima, T.; Haruta, M. *Appl. Catal. B Environ.* **1997**, *12*, 81. https://doi.org/10.1016/S0926-3373(96)00069-0
25. Nikolaev, S.A.; Tsodikov, M.V.; Chistyakov, A.V.; Zharova, P.A.; Ezzgelenko, D.I. *J. Catal.* **2019**, *369*, 501. https://doi.org/10.1016/j.jcat.2018.11.017

26. Hashmi, A.S.K.; Rudolph, M. *Chem. Soc. Rev.* **2008**, *37*, 1766. https://doi.org/10.1039/B615629K
27. Alshammari, A.; Kalevaru, V.N.; Martin, A. *Catalyst* **2016**, *6*, 97. https://doi.org/10.3390/catal6070097
28. Lin, M.; An, B.; Ni, N.; Jikihara, Y.; Nakayama, T.; Honma, T.; Takei, T.; Shishido, T.; Ishida, T.; Haruta, M. *ACS Catal.* **2019**, *9*, 1753. https://doi.org/10.1021/acscatal.8b04272
29. Wilcoxon, J. P.; Abrams, B. L. *Chem. Soc. Rev.* **2006**, *11*, 1162. https://doi.org/10.1039/B517312B
30. Sanabria-Cala J.A.; Conde Rodriguez G.R.; Gauthier, G.H.; Ladeira, L.O.; Laverde Catano, D.A.; Pena Ballesteros, D.Y.; Merchan Arenas, D.R. *Chem. Eng. Trans.* **2018**, *64*, 403. https://doi.org/10.3303/CET1864068
31. Lee, K. X.; Shameli, K.; Yew, Y. P.; Teow, S.-Y.; Jahangirian, H.; Rafiee-Moghaddam, R.; Webster, T. *Int. J. Nanomedicine* **2020**, *15*, 275. https://doi.org/10.2147/IJN.S233789
32. Noruzi, M. *Bioprocess Biosyst. Eng.* **2015**, *1*, 1. https://doi.org/10.1007/s00449-014-1251-0
33. Corma, A.; Garcia, H. *Chem. Soc. Rev.* **2008**, *37*, 2096. https://doi.org/10.1039/B707314N
34. Carabiniero, S. A. C. *Frontiers in Chemistry* **2019**, *7*, 702. https://doi.org/10.3389/fchem.2019.00702
35. del Río, E.; Gaona, D.; Hernández-Garrido, J. C.; Calvino, J. J.; Basallote, M. G.; Fernández-Trujillo, M. J.; Pérez-Omil, A. J.; Gatica J. M. *Journal of Catalysis* **2014**, *318*, 119. http://doi.org/10.1016/j.jcat.2014.07.001
36. Xu, Q.; Kharas, K. C. C.; Datye, A. K. *Catal. Lett.* **2003**, *85*, 229. https://doi.org/10.1023/A:1022106100033
37. Soares, J. M. C., Hall, M.; Cristofolini, M.; Bowker, M. *Catal. Lett.* **2006**, *109*, 103. https://doi.org/10.1007/s10562-006-0064-4
38. Bowker, M.; Nuhu, A.; Soares, J. *Catal. Today* **2007**, *122*, 245. https://doi.org/10.1016/j.cattod.2007.01.021
39. Grisel, R.; Slyconish, J.; Nieuwenhuys, B. *Top. Catal.* **2001**, *16*, 425. https://doi.org/10.1023/A:1016694022941
40. Lin, S.; Vannice, M.A. *Catal. Lett.* **1991**, *10*, 47. https://doi.org/10.1007/BF00764736
41. Carabineiro, S. A. C.; Thompson, D. "Gold Catalysis," in Gold: Science and Applications, eds C. Corti and R. Holliday **2010**, Boca Raton, FL; London, New York, NY: CRC Press; Taylor and Francis Group, 89–122.
42. Onal, Y.; Schimpf, S.; Claus, P. *J. Catal.* **2004**, *223*, 122. https://doi.org/10.1016/j.jcat.2004.01.010
43. Demirel-Gulen, S.; Lucas, M.; Claus, P. *Catal. Today* **2005**, *102*, 166. https://doi.org/10.1016/j.cattod.2005.02.033
44. Demirel, S., Lehnert, K.; Lucas, M.; Claus, P. *Appl. Catal. B Environ.* **2007**, *70*, 637. https://doi.org/10.1016/j.apcatb.2005.11.036
45. Demirel, S.; Lucas, M.; Warna, J.; Murzin, D.; Claus, P. *Top. Catal.* **2007**, *44*, 299. https://doi.org/10.1007/s11244-007-0303-y

46. Shi, L. L.; Liu, K. Z.; Zou, X. H.; Yin, M. S.; Suo, Z. H. *Chinese J. Catal.* **2010**, *31*, 661. https://doi.org/10.3724/SP.J.1088.2010.91137
47. Prati, L.; Villa, A. *Catalysts* **2012**, *2*, 24. https://doi.org/10.3390/catal2010024
48. Koczkur, K. M.; Mourdikoudis, S.; Polavarapu, L.; Skrabalak, S. E. *Dalton Trans.* **2015**, *44*, 17883. https://doi.org/10.1039/C5DT02964C
49. Louie, S. M.; Gorham, J. M.; Tan, J. J.; Hackley, V. A. *Environ. Sci. Nano* **2017**, *4*, 1866. https://doi.org/10.1039/C7EN00411G
50. Ribeiro, A. P. C.; Martins, L. M. D. R. S.; Carabineiro, S. A. C.; Figueiredo, J. L.; Pombeiro, A. J. L. *Molecules* **2017**, *22*, 603. https://doi.org/10.3390/molecules22040603
51. Tofighi, G.; Lichtenberg, H.; Pesek, J.; Sheppard, T. L.; Wang, W.; Schottner, L., Rinke G.; Dittmeyer R.; Grunwaldt, J.-D. *React. Chem. Eng.* **2017**, *2*, 876. https://doi.org/10.1039/C7RE00114B
52. Donoeva, B.; De Jongh, P. E. *ChemCatChem* **2018**, *10*, 989. https://doi.org/10.1002/cctc.201800271
53. Prati, L.; Villa, A. *Acc. Chem. Res.* **2014**, *47*, 855. https://doi.org/10.1021/ar400170j
54. Li, S.; Zhang, Y.; Li, X.; Yang, X.; Li, Z.; Wang, R., Zhu, H. *Catal. Lett.* **2018**, *148*, 328. https://doi.org/10.1007/s10562-017-2231-1
55. Vigneron, F.; Caps, V. *Comptes Rendus Chimie* **2016**, *19*, 192. http://dx.doi.org/10.1016/j.crci.2015.11.015
56. Solsona, B.; García, T.; Hutchings, G.J.; Taylor, S.H.; Makkee, M. *Appl. Catal. A* **2009**, *365*, 222. https://doi.org/10.1016/j.apcata.2009.06.016
57. Tsubota, S.; Haruta, M.; Kobayashi, T.; Ueda, A.; Nakahara, Y. Studies in Surface Science and Catalysis; Elsevier, **1991**, 63, 695. https://doi.org/10.1016/S0167-2991(08)64634-0
58. Cárdenas-Lizana, F.; Pedro, Z. M. D.; Gómez-Quero, S.; Kiwi-Minsker, L.; Keane, M. A. *J. Mol. Catal. Chem.* **2015**, *408*, 138. https://doi.org/10.1016/j.molcata.2015.07.019
59. Behravesh, E.; Kumar, N.; Balme, Q.; Roine, J.; Salonen, J.; Schukarev, A.; Mikkola, J.-P.; Peurla, M.; Aho, A.; Eränen, K.; Murzin, D. Yu.; Salmi, T. *J. Catal.* **2017**, *353*, 223. https://doi.org/10.1016/j.jcat.2017.07.014
60. Li, Q.; Wu, C.; Wang, K.; Wang, X.; Chen, X.; Dai, W.; Fu, X. *Catal. Sci. Technol.* **2022**, *12*, 237. https://doi.org/10.1039/D1CY01829A
61. Moreau, F.; Bond, G. C.; Taylor, A. O. *J. Catal.* **2005**, *231*, 105. https://doi.org/10.1016/j.jcat.2005.01.030
62. Jin, Z.; Song, Y. Y.; Fu, X. P.; Song, Q. S.; Jia, C. J. *Chinese J. Chem.* **2018**, *36*, 639. https://doi.org/10.1002/cjoc.201700731
63. Sunagawa, Y.; Yamamoto, K.; Takahashi, H.; Muramatsu, A. *Catal. Today* **2008**, *132*, 81. https://doi.org/10.1016/j.cattod.2007.12.008
64. Alshammari, A. S. *Catalysts* **2019**, *5*, 402 - including all references therein. https://doi.org/10.3390/catal9050402

65. Pérez, P.; Soria, M. A.; Carabineiro, S. A. C.; Maldonado-Hódar, F. J.; Mendes, A.; Madeira, L. M. *Int. J. Hydrogen Energy* **2016**, *41*, 4670. https://doi.org/10.1016/j.ijhydene.2016.01.037
66. Bond, G.; Thompson, D. *Catal. Rev. Sci. Eng.* **1999**, *41*, 319. https://doi.org/10.1081/CR-100101171
67. Chen, B. B.; Zhu, X. B.; Wang, Y. D.; Yu, L. M.; Lu, J. Q.; Shi, C. *Catal. Today* **2017**, *281*, 512. https://doi.org/10.1016/j.cattod.2016.06.023
68. Azizi, Y.; Pitchon, V.; Petit, C. *Appl. Catal. Gen.* **2010**, *385*, 170. https://doi.org/10.1016/j.apcata.2010.07.010
69. Li, T.; Wang, S. J.; Yu, C. S.; Ma, Y. C.; Li, K. L.; Lin, L. W. *Appl. Catal. Gen.* **2011**, *398*, 150. https://doi.org/10.1016/j.apcata.2011.03.028
70. Carabineiro, S. A. C.; Thompson, D. *"Gold Catalysis," in Gold: Science and Applications*, eds C. Corti and R. Holliday **2010**, Boca Raton, FL; London, New York, NY: CRC Press; Taylor and Francis Group, 89–122.
71. Carabineiro, S. A. C.; Machado, B. F.; Bacsa, R. R.; Serp, P.; Dražić, G.; Faria, J. L.; Figueiredo, J.L. *J. Catal.* **2010**, *273*, 191. https://doi.org/10.1016/j.jcat.2010.05.011
72. Bacsa, R. R.; Dexpert-Ghys, J.; Verelst, M.; Falqui, A.; Machado, B.; Bacsa, W. S.; Chen, P.; Zakeeruddin, S. M.; Graetzel, M.; Serp, P. *Adv. Funct. Mater.* **2009**, *19*, 875. https://doi.org/10.1002/adfm.200801049
73. Carabineiro, S. A. C.; Bogdanchikova, N.; Tavares, P. B.; Figueiredo, J. L. *RSC Adv.* **2012**, *2*, 2957. https://doi.org/10.1039/C2RA00724J
74. Carabineiro, S. A. C., Bogdanchikova, N.; Pestryakov, A.; Tavares, P. B.; Fernandes, L. S. G.; Figueiredo, J. L. *Nanoscale Res. Lett.* **2011**, *6*, 1. https://doi.org/10.1186/1556-276X-6-435
75. Alshammari, A.; Kalevaru, V. N. *Catalytic Application of Nano-Gold Catalysts*; Mishra, N. K., Ed.; InTech, **2016.**
76. Toshima, N.; Yonezawa, T. *New J. Chem.* **1998**, *11*, 1179. https://doi.org/10.1039/A805753B
77. Chen, J.; Fang, W.; Zhang, Q.; Deng, W.; Wang, Y. *Chem. Asian J.* **2014**, *9*, 2187. https://doi.org/10.1002/asia.201402238
78. Elechiguerra, J. L.; Reyes-Gasga, J.; Yacaman, M. J. *J. Mater. Chem.* **2006**, *40*, 3906. https://doi.org/10.1039/B607128G
79. Henry, C. R. *Prog. Surf. Sci.* **2005**, *80*, 92. https://doi.org/10.1016/j.progsurf.2005.09.004
80. Stratakis, M.; Garcia, H. *Chem. Rev.* **2012**, *8*, 4469. https://doi.org/10.1021/cr3000785
81. Chen, M.; Goodman, D. W. *Chem. Soc. Rev.* **2008**, *9*, 1860. https://doi.org/10.1039/B707318F
82. Fierro-Gonzalez, J. C.; Gates, B. C. *Chem. Soc. Rev.* **2008**, *9*, 2127. https://doi.org/10.1039/B707944N
83. Sanchez, A.; Abbet, S.; Heiz, U.; Schneider, W.-D.; Häkkinen, H.; Barnett, R. N.; Landman, U. *J. Phys. Chem. A* **1999**, *48*, 9573. https://doi.org/10.1021/jp9935992
84. Farnesi Camellone, M.; Kowalski, P. M.; Marx, D. *Phys. Rev. B* **2011**, *84*, 035413.

https://doi.org/10.1103/PhysRevB.84.035413
85. Nasrallah, H. O.; Min, Y.; Lerayer, E.; Nguyen, T.-A.; Poinsot, D.; Roger, J.; Brandès, S.; Heintz, O.; Roblin, P.; Jolibois, F.; Poteau, R.; Coppel, Y.; Kahn, M. L.; Gerber, I. C.; Axet, M. R.; Serp, P.; Hierso, J.-C. *JACS Au* **2021**, *2*, 187. https://doi.org/10.1021/jacsau.0c00062
86. Sankar, M.; He, Q.; Engel, R. V.; Sainna, M. A.; Logsdail, A. J.; Roldan, A.; Willock, D. J.; Agarwal, N.; Kiely, Ch. J.; Hutchings, G. J. *Chem. Rev.* **2020**, *120*, 3890. https://doi.org/10.1021/acs.chemrev.9b00662
87. Liu, X. Y.; Wang, A.; Zhang, T.; Mou, C.-Y. *Nano Today* **2013**, *8*, 403. https://doi.org/10.1016/j.nantod.2013.07.005
88. Meyer, R.; Lemire, C.; Shaikhutdinov, Sh. K.; Freund, H.-J. *Gold Bull.* **2004**, *37*, 72. https://doi.org/10.1007/BF03215519
89. Villa, A.; Dimitratos, N.; Chan-Thaw, C. E.; Hammond, C.; Veith, G. M.; Wang, D.; Manzoli, M.; Prati, L.; Hutchings, G. J. *Chem. Soc. Rev.* **2016**, *45*, 4953. https://doi.org/10.1039/C5CS00350D
90. Ishida, T.; Koga, H.; Okumura, M.; Haruta, M. *Chem. Rec.* **2016**, *16*, 2278. https://doi.org/10.1002/tcr.201600046
91. Kung, M. C.; Davis, R. J.; Kung, H. H. *J. Phys. Chem. C* **2007**, *111*, 11767. https://doi.org/10.1021/jp072102i
92. Mourdikoudis, S.; Pallares, R. M.; Thanh, N. T. K. *Nanoscale* **2018**, 10, 12871. https://doi.org/10.1039/C8NR02278J
93. Notar Francesco, I.; Fontaine-Vive, F.; Antoniotti, S. *ChemCatChem* **2014**, 6, 2784. https://doi.org/10.1002/cctc.201402252
94. Inkson, B. J. *Materials Characterization Using Nondestructive Evaluation (NDE) Methods*; Elsevier, **2016**; 17–43.
95. Shnoudeh, A. J.; Hamad, I.; Abdo, R. W.; Qadumii, L.; Jaber, A. Y.; Surchi, H. S.; Alkelany, S. Z. *Biomaterials and Bionanotechnology*; Elsevier, **2019**; 527–612.
96. *Metal Nanoclusters in Catalysis and Materials Science: The Issue of Size Control*, *1st ed.*; Corain, B., Schmid, G., Toshima, N., Eds.; Elsevier: Amsterdam; Boston, **2008.**
97. Shard, A. G. A *J. Phys. Chem.* **2012**, *31*, 16806. https://doi.org/10.1021/jp305267d
98. Casaletto, M. P.; Longo, A.; Martorana, A.; Prestianni, A.; Venezia, A. M. *Surf. Interface Anal.* **2006**, *4*, 215. https://doi.org/10.1002/sia.2180
99. *Handbook of X-Ray Photoelectron Spectroscopy: A Reference Book of Standard Spectra for Identification and Interpretation of XPS Data*; Moulder, J. F., Stickle, W. F., Sobol, P. E., Bomben, K. D., Chastain, J., King Jr., R. C., Physical Electronics, Incorporation, Eds.; Physical Electronics: Eden Prairie, Minn., **1995**.
100. Brunauer, S.; Emmett, P. H.; Teller, E. *J. Am. Chem. Soc.* **1938**, *60*, 309. https://doi.org/10.1021/ja01269a023
101. Sing, K.S.W. *Adv. Colloid Interface Sci.* **1998**, *76–77*, 3. https://doi.org/10.1016/S0001-8686(98)00038-4
102. Chiorino, A.; Manzoli, M.; Menegazzo, F.; Signoretto, M.; Vindigni, F.; Pinna, F.; Boccuzzi, F. *J. Catal.* **2009**, *262*, 169. https://doi.org/10.1016/j.jcat.2008.12.017
103. Berndt, H.; Pitsch, I.; Evert, S.; Struve, K.; Pohl, M. M.; Radnik, J.; Martin, M. *Appl. Catal. A* **2003**, *244*, 169.

https://doi.org/10.1016/S0926-860X(02)00575-6
104. Iizuka, Y.; Fujiki, H.; Yamauchi, N.; Chijiiwa, T.; Arai, S.; Tsubota, S.; Haruta, M. *Catal. Today* **1997**, *36*, 123. https://doi.org/10.1016/S0920-5861(96)00204-0
105. Egerton, R. F.; Watanabe, M. *Ultramicroscopy* **2018**, *193*, 111. https://doi.org/10.1016/j.ultramic.2018.06.013
106. Fujita, T.; Zysman, M.; Elgrabli, D.; Murayama, T.; Haruta, M.; Lanone, S.; Ishida, T.; Boczkowski, J. *Sci Rep.* **2021**, *11*, 23129. https://doi.org/10.1038/s41598-021-02419-4
107. Meijerink M. J.; de Jong K. P.; Zečević J. *J Phys Chem C* **2020**, 124, 2202. https://doi.org/10.1021/acs.jpcc.9b10237
108. Campos, C. H.; Urbano, B. F.; Torres, C. C.; Alderete, J. A. *J. Chem.* **2017**, 1, 7941853. https://doi.org/10.1155/2017/7941853
109. Ping, Y.; Xu, S.; Kong, W. *Acc. Chem. Res.* **2025**, *58*, 2477. https://doi.org/10.1021/acs.accounts.5c00355
110. Giorgi, P. D. ; Liautard, V.; Pucheault, M.; Antoniotti, S. *Eur. J. Org. Chem.* **2018**, *11*, 1307. https://doi.org/10.1002/ejoc.201800064
111. Giorgi, P. D.; Miedziak, P. J.; Edwards, J. K.; Hutchings, G. J.; Antoniotti, S. *ChemCatChem* **2017**, *9*, 70. https://doi.org/10.1002/cctc.201601644
112. Plevova, K.; Michelet, V.; Antoniotti, S. *Commun. Chem.* **2024**, *7*, 248. https://doi.org/10.1038/s42004-024-01336-7
113. Tomás-Mendivil, E.; Starck, J.; Ortuno, J.-C.; Michelet, V. *Org. Lett.* **2015**, 17, 6126. https://doi.org/10.1021/acs.orglett.5b03146
114. Ning, L.; Liao, S.; Liu, X.; Guo, P.; Zhang, Z.; Zhang, H.; Tong, X. J. Catal. 2018, 364, 1. https://doi.org/10.1016/j.jcat.2018.04.030
115. Zantioti-Chatzouda, E.-M.; Kotzabasaki, V.; Stratakis, M. *J. Org. Chem.* **2022**, *87*, 8525. https://doi.org/10.1021/acs.joc.2c00627
116. Soulé, J.-F.; Miyamura, H.; Kobayashi. S. *Chem. Asian J.* **2013**, *8*, 2614. https://doi.org/10.1002/asia.201300733
117. Soulé, J.-F.; Miyamura, H.; Kobayashi, S. *Chem. Commun.* **2013**, 49, 355. https://doi.org/10.1039/C2CC36213A
118. Wu, S.; Sun, W.; Chen, J.; Zhao, J.; Cao, Q.; Fang, W.; Zhao, Q. *J. Catal.* **2019**, *377*, 110. https://doi.org/10.1016/j.jcat.2019.07.027
119. C. He, Q.-J. Wu, M.-J. Mao, Y.-H. Zou, B.-T. Liu, Y.-B. Huang, R. Cao. *CCS Chemistry* **2020,** *3*, 2368. https://doi.org/10.31635/ccschem.020.202000460
120. Fragkiadakis, M.; Kidonakis, M.; Zorba, L.; Stratakis, M. *Adv. Synth. Catal.* **2020**, *362*, 964. https://doi.org/10.1002/adsc.201901451
121. Naapuri, J. M.; Losada-Garcia, N., Deska, J.; Palomo, J. M. *Nanoscale* **2022**, *14*, 5701. https://doi.org/10.1039/D2NR00361A
122. Xu, Y.; Fei, J.; Li, G.; Yuan, T.; Xu, X.; Li, J. *Angew. Chem. Int. Ed.* **2019,** *58*, 5572. https://doi.org/10.1002/anie.201813771
123. Chen, J.; Ma, Q.; Li, M.; Chao, D.; Huang, L.; Wu, W.; Fang, Y.; Dong, S. *Nat. Commun.* **2021,** *12*, 3375. https://doi.org/10.1038/s41467-021-23737-1
124. Zhang, H.; Liang, X.; Han, L.; Li, F. *Small* **2018,** *14*, 1803256. https://doi.org/10.1002/smll.201803256

125. Deshmukh, A. R.; Aloui, H.; Kim, B. S. *Chem. Eng. J.* **2021,** *421*, 127859. https://doi.org/10.1016/j.cej.2020.127859
126. Miyamura, H.; Suzuki, A.; Yasukawa, T.; Kobayashi, S. *Adv. Synth. Catal.* **2015**, *357*, 3815. https://doi.org/10.1002/adsc.201500529
127. Morales-Guio, C. G.; Cave, E. R.; Nitopi, S. A.; Feaster, J. T.; Wang, L.; Kuhl, K. P.; Jackson, A.; Johnson, N. C.; Abram, D. N.; Hatsukade, T.; Hahn, C.; Jaramillo, T. F. *Nat. Catal.* **2018**, *1*, 764. https://doi.org/10.1038/s41929-018-0139-9
128. Qi, M.Y.; Wu, H.K.; Anpo, M.; Tang, Z.-R.; Xu, Y.-J. *Nano Res.* **2022**, *15*, 9967. https://doi.org/10.1007/s12274-022-4176-y

Authors' Biographies

K. Plevova received her PhD from Slovak University of Technology in Bratislava (Slovakia) in 2015, under the supervision of Professor V. Milata. After her doctorate, she completed postdoctoral research in the laboratories of Profesor S. Thorimbert (UPMC, Paris, France), Professor R. Sebesta (PriFUK, Bratislava, Slovakia) and Professor J. Cossy (ESPCI, Paris, France). In 2021, she became a research assistant at Université Côte d'Azur, Nice (France), in the groups of Professor V. Michelet and Dr. S. Antoniotti. In September 2023, she was appointed Assistant Professor at Université Côte d'Azur as a member of the "*Green and Sustainable Chemistry*" research group at Nice Institute of Chemistry (ICN). Her research focuses on the development of new synthetic strategies for organic chemistry respecting the rules of green and sustainable chemistry, including synthesis and use of supported nanoparticles or nanocages for the synthesis of biologically active compounds or molecules with olfactory properties.

S. Antoniotti is Research Director at CNRS and Vice-President of Université Côte d'Azur in charge of the Initiative of Excellence. He was awarded a PhD in chemical sciences in 2003 from Université Nice Sophia Antipolis, then carried out postdoctoral research in Jon Dordick's lab at Rensselaer Polytechnic Institute (NY, USA), and Jean-Pierre Genet's lab at ENSCP (now Chimie Paristech). In 2005 he was appointed CNRS research fellow at the future Nice Institute of Chemistry (ICN). He obtained accreditation to supervise research (HDR) in 2008 and founded his research group in 2012. Promoted to research director in 2017, he has since led three research themes in sustainable chemistry and fragrance chemistry. In 2016 he was elected president of the scientific board of the ERINI platform in Grasse, and in 2017 he created the Center for Creativity and Innovation in Odorant Sciences, now an Innovation and Partnership Institute. He joined the board of the University's IdEx in 2020 as strategic director and was appointed Vice-President in 2021.

